Repeatability of adaptation in sunflowers: genomic regions harbouring inversions also drive adaptation in species lacking an inversion

Shagheyegh Soudi[1+], Mojtaba Jahani[1,2+], Marco Todesco[2,3,4], Gregory L. Owens[5], Natalia Bercovich[2], Loren H. Rieseberg[2], Sam Yeaman[1,*]

+Joint first-authors

Author affiliations:

1. Department of Biological Sciences, University of Calgary, 2500 University Drive NW, Calgary, Canada, T2N 1N4
2. Department of Botany, University of British Columbia, 6270 University Blvd, Vancouver, Canada, V6T 1Z4
3. Michael Smith Laboratories, University of British Columbia, 6270 University Blvd, Vancouver, Canada, V6T 1Z4
4. Irving K. Barber Faculty of Science, University of British Columbia Okanagan, 3187 University Way, Kelowna, Canada, V1V 1V7
5. Department of Biology, University of Victoria, 3800 Finnerty Rd, Victoria, Canada, V8P 5C2

*corresponding author: Sam Yeaman, samuel.yeaman@ucalgary.ca

Abstract

Local adaptation commonly involves alleles of large effect, which experience fitness advantages when in positive linkage disequilibrium (LD). Because segregating inversions suppress recombination and facilitate the maintenance of LD between locally adapted loci, they are also commonly found to be associated with adaptive divergence. However, it is unclear what fraction of an adaptive response can be attributed to inversions and alleles of large effect, and whether the loci within an inversion could still drive adaptation in the absence of its recombination-suppressing effect. Here, we use genome-wide association studies to explore patterns of local adaptation in three species of sunflower: *Helianthus annuus*, *H. argophyllus*, and *H. petiolaris*, which each harbour a large number of species-specific inversions. We find evidence of significant genome-wide repeatability in signatures of association to phenotypes and environments, which are particularly enriched within regions of the genome harbouring an inversion in one species. This shows that while inversions may facilitate local adaptation, at least some of the loci involved can still make substantial contributions without the benefit of recombination suppression. While a large number of genomic regions show evidence of repeated adaptation, most of the strongest signatures of association still tend to be species-specific, indicating substantial genotypic redundancy for local adaptation in these species.

Introduction

The genetic basis of local adaptation is sometimes highly repeatable, with examples of large effect genes driving responses in multiple species, such as *FT* affecting flowering time in numerous plants (Izawa 2007; Auge et al. 2019) or *Mc1r* driving colour polymorphisms in vertebrates(Manceau et al. 2010; Rosenblum et al. 2014). Local adaptation can also be repeated for polygenic traits, with significant patterns of similar association found across many loci for comparisons of conifers (Yeaman et al. 2016), maize and its wild relative teosinte (Tittes et al. 2021; Wang et al. 2021), and *Brassicaceae* (Bohutínská et al. 2021), to name a few. While we have a growing number of examples of repeatability in the basis of adaptation, it is also interesting to know if species use different genes to adapt to the same selection pressure. Genotypic redundancy – the potential for many genotypes to yield a given phenotype -- is one critical factor affecting the repeatability of adaptation, as high redundancy would be expected to result in lower repeatability (Yeaman et al. 2018). Another critical factor affecting repeatability

is shared standing variation, whether present due to introgression or incomplete lineage sorting. In either case, variants shared among lineages are much more likely to contribute to a repeated response than new mutations (MacPherson and Nuismer 2018; Ralph and Coop 2015). Consistent with this, Bohutínská and colleagues (2021) found that repeatability was negatively related to phylogenetic distance. While we are now accumulating more studies about the repeatability of adaptation, we still have very few examples and much remains unknown about the relative importance of these factors (Yeaman 2022).

Inversions have been implicated in local adaptation in many species (Wellenreuther and Bernatchez 2018), likely due to their effect to suppress recombination between any causal loci within their bounds (Rieseberg 2001; Noor et al. 2001; Kirkpatrick and Barton 2006). Despite mounting evidence of their importance in adaptation, it is unclear how inversions may covary with repeatability of adaptation among species. If most alleles have small effects relative to migration rate and can only contribute to local adaptation via the benefit of the recombination-suppressing effect of an inversion, then we would expect little repeatability at the site of an inversion – other species lacking the inversion would not tend to use that same region for adaptation. On the other hand, if some loci are particularly important for local adaptation and regularly yield mutations of large effect, with these patterns being conserved among species, repeatability within regions harbouring inversions may be substantial.

Here, we explore the repeatability of local adaptation in three species of sunflowers, *Helianthus annuus*, *Helianthus argophyllus* and *Helianthus petiolaris* (Figure 1), which harbour large regions of suppressed recombination ("haploblocks"), most of which are likely inversions, and are often associated with adaptive traits (Todesco et al. 2020). *Helianthus annuus*, the common sunflower, is the closest wild relative of cultivated sunflower, which was domesticated from it around 4,000 years ago (Blackman et al. 2011). Populations of *H. annuus* are distributed throughout the central and western USA and generally found on mesic soils, but can grow in a variety of disturbed or extreme habitats, such as semi-desertic or frequently flooded areas, as well as salt marshes. *Helianthus petiolaris*, the prairie sunflower, prefers sandier soils, and ecotypes of this species are adapted to sand sheets and sand dunes (Ostevik et al. 2016). Here we include samples from two subspecies: *H. petiolaris ssp. petiolaris*, which is commonly found in

87 the southern Great Plains, and *H. petiolaris ssp. fallax*, which is limited to more arid regions in
88 Colorado, Utah, New Mexico and Arizona (Heiser et al. 1969). *Helianthus petiolaris* and *H.*
89 *annuus* have broad and overlapping distributions throughout the central and western United
90 States and appear to have adapted to similar changes in temperature, moisture and photoperiod
91 regimes. There is also evidence indicating *H. annuus* and *H. petiolaris* have likely been
92 exchanging genes during much of their history of divergence (Strasburg and Rieseberg 2008),
93 although partially isolated by strong pre- and post-zygotic barriers (Sambatti et al. 2012). The
94 third species, *Helianthus argophyllus*, the silverleaf sunflower, is found exclusively in the
95 southeast coast of Texas and includes both an early flowering ecotype on the coastal barrier
96 islands and a late flowering ecotype inland (Moyers and Rieseberg 2016; Todesco et al. 2020).
97 *H. argophyllus* is thought to have undergone cycles of sympatry and allopatry with *H.*
98 *annuus* and *H. petiolaris* over time, but currently only overlaps with *H. annuus,* which is likely
99 recent (Heiser, 1951).
100
101 Using broad sampling across the ranges of these species (Figure 1), we study the genomic
102 basis of local adaptation by conducting genome-wide scans for associations with climatic and
103 soil environmental variables and phenotypes measured in a common garden. An inherent
104 problem in studying the basis of local adaptation is accounting for the covariance between
105 genome-wide population genetic structure and environment. When the selection pressure driving
106 local adaptation tends to parallel a main axis of demographic expansion or isolation by distance,
107 neutral alleles will have spatial patterns resembling those of causal alleles. Methods that do not
108 correct for population structure have large numbers of false positives because allele frequencies
109 at neutral loci tend to correlate with the environment more than expected by chance (Lotterhos
110 and Whitlock 2014). By contrast, methods that use structure correction tend to suffer from false
111 negatives because the causal loci have similar patterns of allele frequency variation as the
112 genomic background, and so their statistical signatures are decreased (DeRaad et al. 2021).
113 When a non-corrected approach is applied to multiple species, the false positive problem can be
114 mitigated when testing for loci that contribute to repeated adaptation, as the same gene should
115 not tend to be a false positive in multiple species more often than expected by chance (Yeaman
116 et al. 2016). Here we use a conventional GWAS approach with structure correction to study the
117 basis of phenotypes, which vary both within and among populations, and use an uncorrected

approach to test association to environment, which only varies among populations. For the environmental association portions of the study, we also explore the effect of structure correction in some analyses, to contrast the false negative vs. false positive problem inherent in each approach. We apply these approaches individually to *H. annuus*, *H. argophyllus*, and the two *H. petiolaris* subspecies, and make pairwise and higher-order comparisons among combinations of these four lineages to study repeatability.

Our overall aim is to characterize the extent of repeatability of local adaptation for different traits and environments, and explore the importance of various factors that may drive differences in repeatability. We begin by using the strength of phenotype-environment correlations to identify which environmental variables are most important in driving local adaptation within each species, and use an index to quantify the relative similarity in these patterns among pairs of species. We then use methods similar to Yeaman et al. (2016) to identify regions of the genome that exhibit greater similarity in signatures of association among pairs of lineages than expected by chance, and explore how the number and total size of these regions covaries with the index of similarity in environmental importance. We also explore whether these regions of repeated adaptation tend to covary with patterns of shared standing variation and test if they are enriched within previously identified haploblocks, to explore the role of inversions in adaptation. We then identify candidate genes that show particularly strong signatures of repeated adaptation across multiple lineages and test whether they tend to share common Gene Ontology terms indicating similar function. Finally, based on the number of signatures of adaptation that are shared vs. non-shared among lineages, we estimate the number of regions genome-wide that could potentially contribute to local adaptation for each variable and phenotype, which is related to the genotypic redundancy. Taken together, our results show that local adaptation in sunflowers tends to involve both strong repeatability at a small number of genes, often associated with inversions, coupled with high redundancy and non-repeated responses across a much larger number of loci.

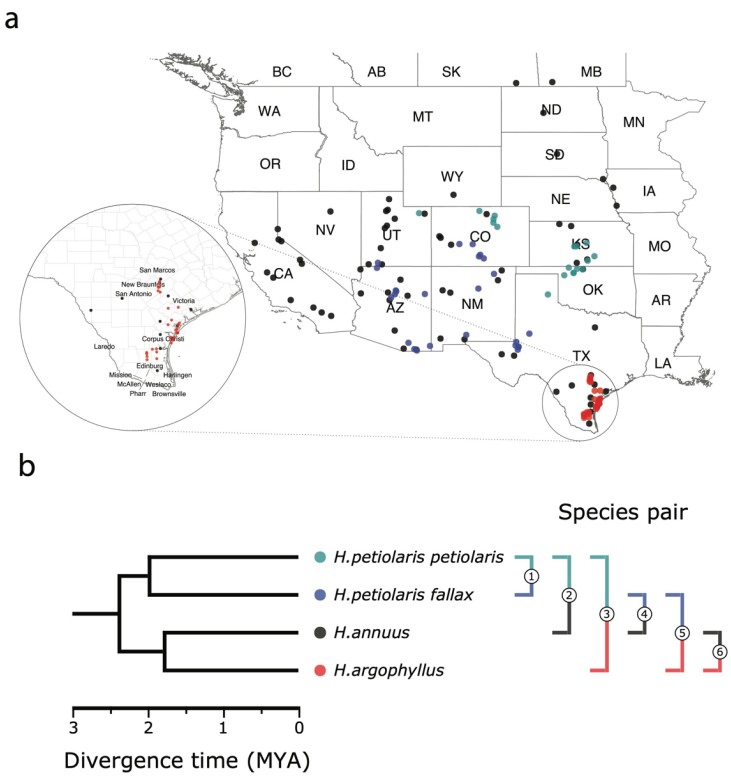

Figure 1. Sampling sites and phylogenetic relationship among surveyed species. (a), sampling locations of wild sunflower populations studied in the present study. (b) phylogenetic relationship of the four (sub-)species. Numbered brackets represent the six pairwise comparisons performed in this study.

Results

Local adaptation at the phenotypic level. The four taxa vary considerably in the breadth of environmental variation spanned by their respective ranges, with *H. annuus* spanning the widest niche and *H. argophyllus* spanning the narrowest (Figure 2A). Local adaptation is quite pronounced, as exhibited by strong correlations for many combinations of phenotypes and environmental variables (Figure S1). To quantify the similarity in patterns of local adaptation among pairs of species, for each environmental variable we calculate an index we refer to as the Similarity in Phenotype-Environment Correlation (SIPEC), which is maximized when both species have strong correlations with the environmental variable across many phenotypes (see

Methods). To prevent heavily weighting the contribution of multiple highly correlated phenotypes, we fit a principal components analysis to the phenotypes and used the resulting axes to calculate SIPEC. We find the largest values of SIPEC for temperature variables and the smallest values for soil types, and generally find higher values for comparisons between the *petiolaris* subspecies (Figure S2).

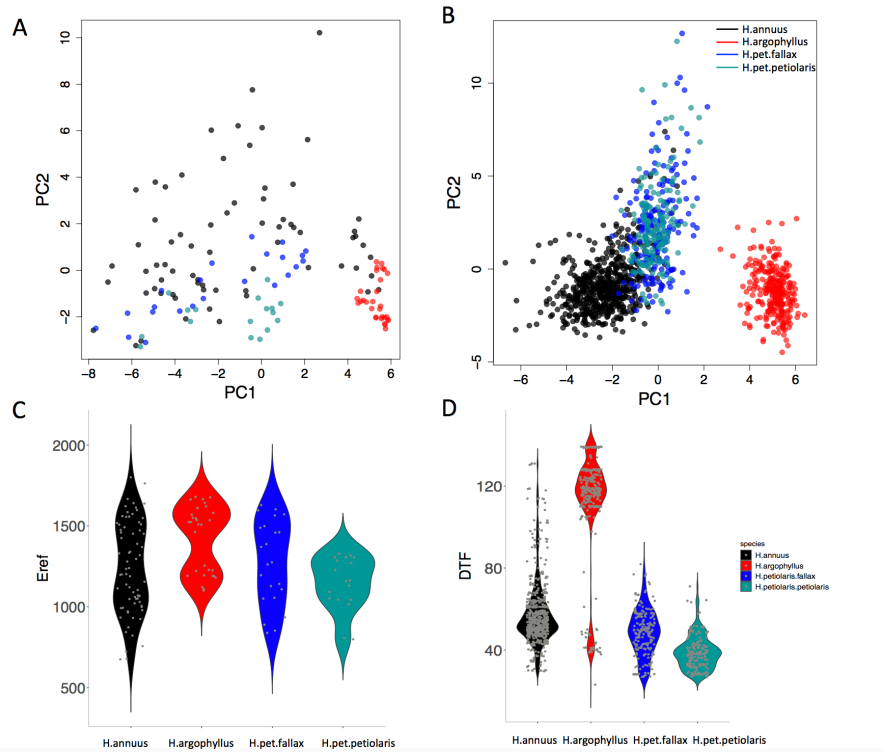

Figure 2. The range of environmental and phenotypic overlaps among studied species. Principle component analysis (PCA) indicating how different species span the range of environmental and phenotypic space, respectively (a, b). Violin plots show two examples of variation in environment (Hargreaves reference evapotranspiration index; Eref) and phenotype (Days to Flower; DTF) within and among the taxa (c,d).

Genome-wide analysis of repeated local adaptation. To search for regions of the genome with signatures of repeated adaptation in multiple taxa, we first identified windows of the genome within each species that showed strong signatures of association to either phenotype (GWAS) or

environment (GEA), referred to as "top candidate" windows. To identify Windows of Repeated Association (WRAs) between pairs of species, we then assessed whether top candidate windows identified in one focal taxon also tended to be enriched for strong signatures of association to the same environment or phenotype in each of the other taxa (using the null-W test, which tends to be more sensitive than just finding the overlap between the top candidate windows; See Methods). As recombination rate can affect the sensitivity of these kinds of window-based genome scans (Booker et al. 2020), the identification of WRAs was conducted after binning windows by recombination rate, although in many cases we did not observe substantial differences in the null distributions among these bins (*e.g.*, Figure S3). This analysis revealed many windows with signatures of repeated association, with the strongest repeated signature found for Number of Frost-Free Days (NFFD; Figure 3A; S4), but also showed that many of the windows with the strongest association in one species did not have strong signatures in other species (Figure 3B).

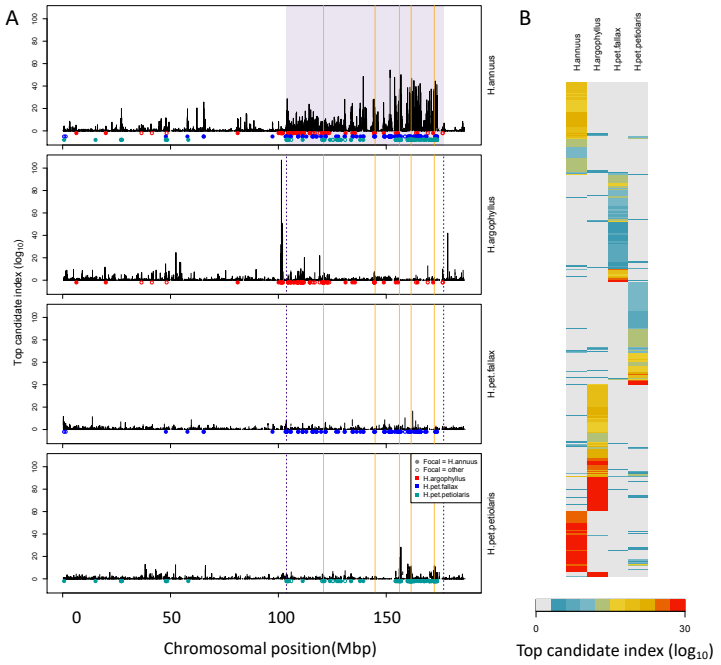

Figure 3. Signatures of association for Number of Frost-Free Days (NFFD) in the four taxa on chromosome 15 (A) and genome-wide (B). Panel A shows Windows of Repeated Association (WRAs; coloured bars) for comparisons between the focal speces, *H. annuus*, and each of the other 3 taxa, with the haploblocks in *H. annuus* shaded in violet and the regions with significant

204 PicMin hits as vertical orange lines. Panel B shows the value of the top candidate index for each
205 of the 1000 windows with the strongest signatures of association in at least one species, ordered
206 by clustering to group windows with similar patterns across multiple species.
207
208 Under the null hypothesis that all regions of the genome evolve neutrally due to drift and
209 independently in each species, ~5% of the top candidate windows identified in one species
210 would be expected to fall into the tail of the null distribution of another species (i.e. be classified
211 as WRAs). While we find significantly more WRAs than the 5% expected by chance, ranging
212 from 6.3% to 44.1% (mean = 14.5%; Figure S4), multiple factors can violate the assumptions of
213 this test and increase the proportion of windows classified as WRAs. Most importantly,
214 similarity in signatures of association can be driven by shared ancestral variation or ongoing
215 introgression, and this must always be considered as an alternative explanation. It is clear that
216 most regions of the genome harbour some shared standing variation between all 6 pairwise
217 comparisons of the taxa, whether due to segregating ancestral variation or introgression, based
218 on an index quantifying the proportion of shared to non-shared SNPs in each window (Figure
219 S5). However, we do not find consistent differences in the amount of shared standing variation
220 within windows when comparing WRAs with the rest of the genome (Figure S5). Thus, while
221 introgression may make subtle contributions to WRAs, a lack of increased shared standing
222 variation in the significant windows suggests that it is not a primary driver of these patterns.
223 A second source of inflation in the number of WRAs is due to hitchhiking: if a given
224 locus is a true positive driving adaptation, LD with other windows in tight physical linkage will
225 result in spurious correlations causing them to also be classified as WRAs increasing the
226 genome-wide proportion above 5%, and this effect will be particularly exaggerated in
227 haploblocks. To control for this, we binned neighbouring WRAs together that exhibited high LD
228 (>95th percentile) over short spans of the genome (<1 cM) in either species, yielding regions we
229 refer to as Clusters of Repeated Association (CRAs). While this clustering method should
230 provide a partial control for the effect of hitchhiking, we note that the number of CRAs cannot be
231 taken as a reliable estimate of the number of independent targets of natural selection. Instead, we
232 treat the number and size of these CRAs as proxies for the relative genome-wide similarity in
233 association between each pair of species, and conduct downstream analyses to test hypotheses
234 about the factors driving local adaptation.

235 CRAs varied in number and size across the 6 pairwise-species comparisons, with
236 particularly large CRAs identified at the sites of known haploblocks (Todesco et al. 2020). For
237 CRAs identified for phenotypic associations, their extent ranged from 168 clusters spanning
238 48,524,903 bp (covering only 1.6% of the genome) in *H.argophyllus-H.pet.petiolaris* to a
239 maximum of 1,667 clusters spanning 426,409,647 bp (14.2 % of the genome) in *H. pet.*
240 *petiolaris-H. pet. fallax* (Figure S6). CRAs identified for environmental variables tended to be
241 more numerous and cover a larger region of the genome, varying from 1154 clusters comprising
242 15% of the total genome for *H. argophyllus-H. pet. fallax* up to 2,260 distinct clusters covering
243 29% of the genome between *H. petiolaris* subspecies (Figure S7). When we use an approach that
244 corrects for population structure in the genotype-environment association tests (Baypass), we
245 find substantially reduced numbers of CRAs (Figure S8), likely due to reduced power to detect
246 true positive causal loci when population structure covaries with environment (as true positives
247 do not "stand out" relative to the genomic background).
248
249 **Repeated association in the genome reflects patterns at the phenotypic level.** If natural
250 selection is driving repeated patterns of local adaptation in the genomes of two species, we
251 should see greater similarity for associations with environmental variables that are also strongly
252 associated with phenotypic variation in both species. Consistent with this prediction, we found
253 that environmental variables with a high SIPEC index (i.e. high correlation with phenotypes;
254 Figure S2) also tended to have a larger number of CRAs in all comparisons (Figure 4), with
255 higher repeatability at both the phenotype and genome level for temperature-related variables
256 and much lower repeatability for soil-related variables. Unfortunately, given the non-
257 independence of environmental variables it is not possible to conduct a formal significance test
258 of these patterns. In all cases, the number of CRAs exhibited a weak negative relationship with
259 the index of standing variation, with environmental variables that had the greatest number of
260 CRAs having the lowest relative amounts of shared standing variation (Figure S9). This suggests
261 that the observed similarity in patterns of association among species is not being strongly driven
262 by incomplete lineage sorting or introgression, as we would expect a positive relationship
263 between the index of shared standing variation and the number of CRAs. We found similar but
264 weaker patterns in the association between SIPEC and size of CRAs (Figure S10), which may
265 reflect comparatively greater contribution of haploblocks driving patterns with size rather than

number (i.e. if a particularly large haploblock is a CRA, then that variable will have a particularly large value relative to its actual importance for local adaptation).

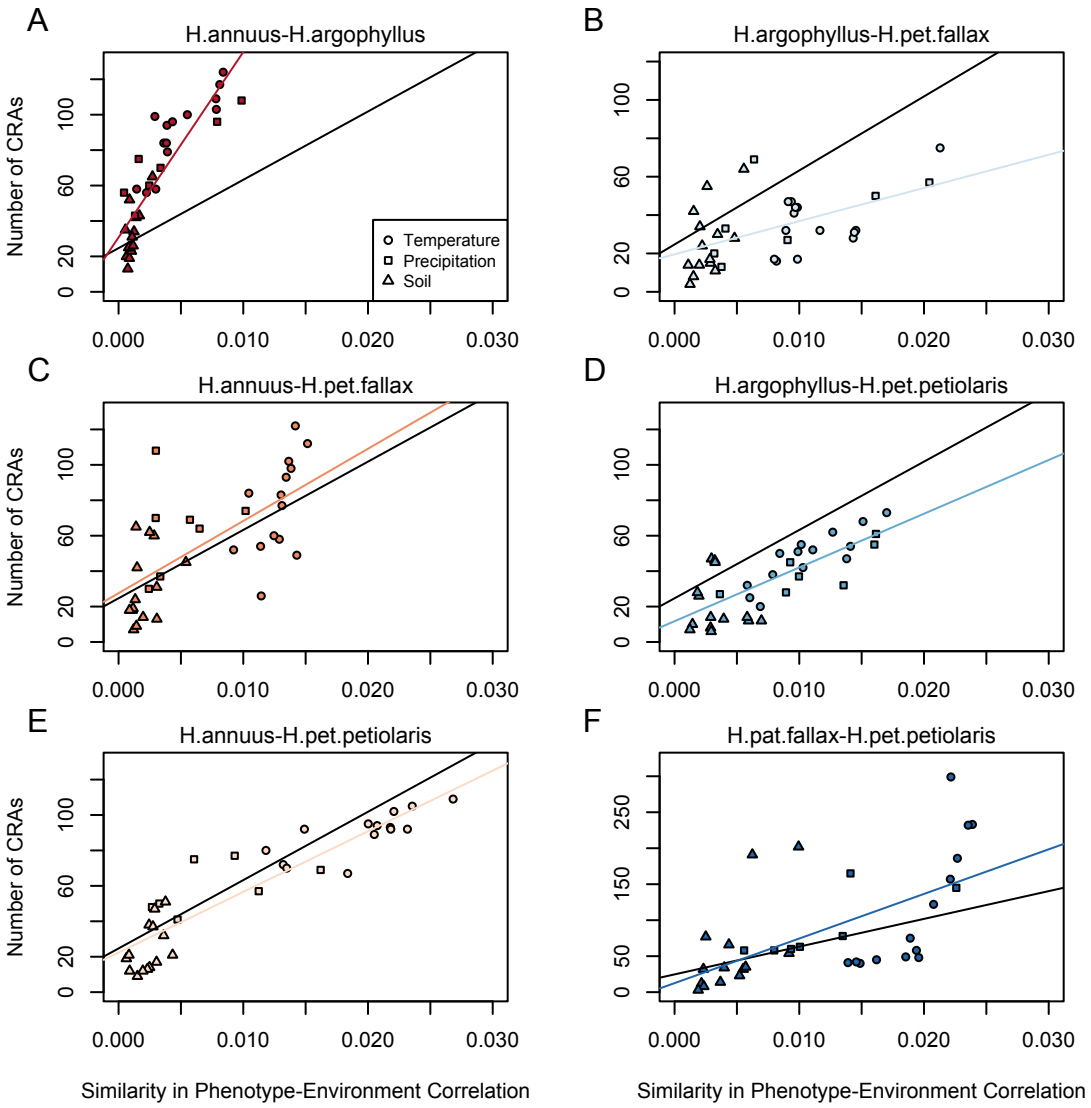

Figure 4. Relationship between mean Similarity in Phenotype-Environment Correlation (SIPEC) and number of Clusters of Repeated Association (CRAs). Each panel includes both a linear model fit to the data within the panel (coloured lines), and a linear model fit to all data simultaneously (black lines) for comparison.

Overlap of signatures of repeated association with low recombination haploblocks. Inversions can facilitate local adaptation by suppressing recombination between locally adapted alleles within the inverted vs. ancestral haplotypes (Kirkpatrick and Barton 2006). If a given species exhibits a signature of association to environment at a segregating inversion, it is interesting to test whether similar signatures of association are found in other species at the same region of the genome that lack a segregating inversion. This would suggest that particularly strong selection is acting on this region, as signatures of association can still evolve even without the recombination suppressing effect of the inversion. While not all of the low-recombination haploblocks identified by Todesco et al. (2020) have been validated as inversions, for simplicity we treat each haploblock as representative of a segregating inversion. The majority of these haploblocks are present as segregating variation in only one of the three species, but when they occur in *H. petiolaris*, they tend to be found as segregating variation within both subspecies. Thus, if we find significant enrichment of the regions of repeated association (WRAs and CRAs) within haploblocks, this suggests that both the species with a segregating inversion and the species lacking an inversion are using this region of the genome to drive local adaptation. As a first test of this relationship, we assessed two-way contingency tables for whether top candidate windows within a species were also significant windows of repeated association (WRA/non-WRA) and whether they fell within haploblocks (yes/no). This approach controls for the potential enrichment of top candidate windows within haploblocks relative to the rest of the genome and asks if the rate of WRAs within haploblocks is higher. For most phenotypes and environments, we found that the proportion of WRAs in haploblocks was much higher than for non-WRAs (Figure 5). Across all species comparisons and environmental/phenotypic variables, a total of 310 contrasts showed significant enrichment for WRAs in haploblocks, compared to only 23 contrasts showing a significantly higher proportion of non-WRAs in haploblocks. In *H. argophyllus*, while non-WRA top candidates tended to fall within haploblocks less commonly than in the other taxa, WRAs tended to be very strongly enriched within haploblocks (Figure 5B). As a follow-up, we also tested whether CRAs were enriched within haploblocks (without controlling for whether top candidate windows also tended to be enriched), also finding strongly significant enrichment of CRAs within haploblocks for many traits and environments (Figure S6C & D). Broad patterns revealed by these analyses are similar, as both show that regions with haploblocks tend to be enriched for signatures of association to environment in species lacking

308 the haploblock. It is noteworthy that few significant signatures of enrichment in haploblocks
309 were found for *H. petiolaris petiolaris* vs. *H. petiolaris fallax* (Figure S6C & D), perhaps
310 because extensive introgression across non-locally adapted regions of the genome obscures true
311 signal.
312

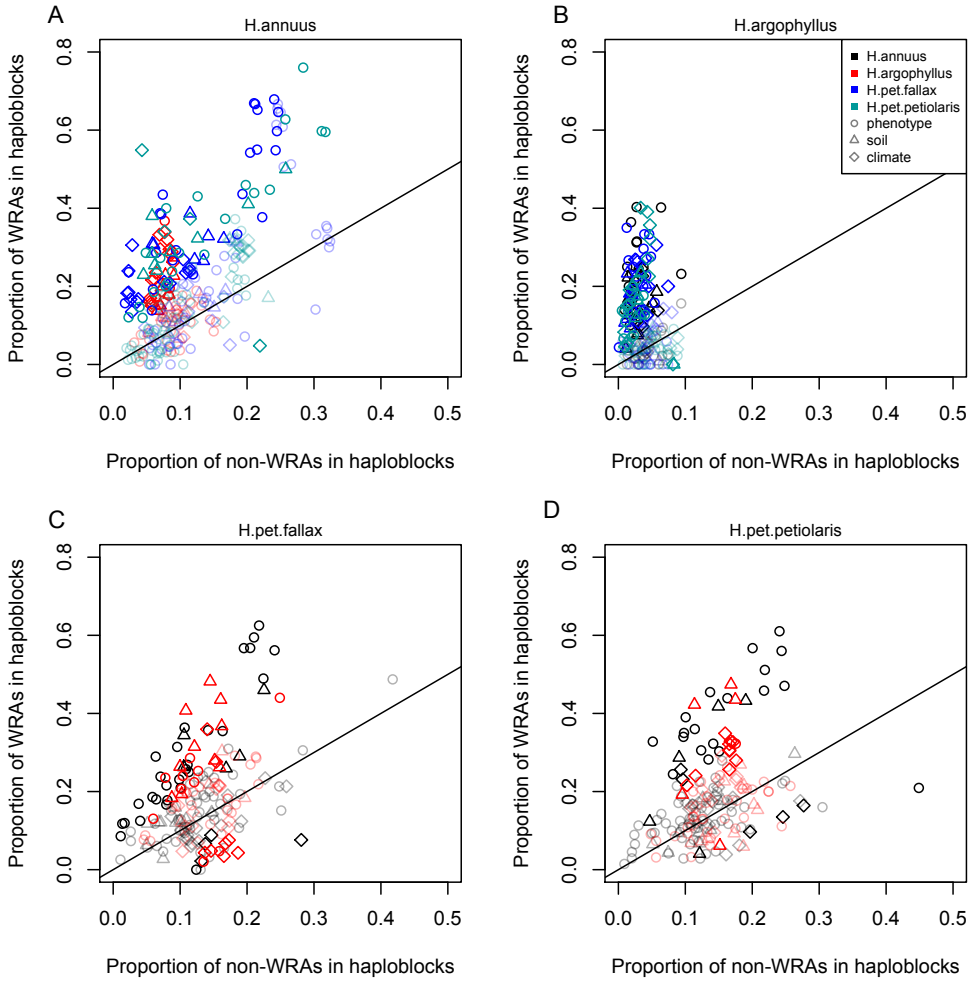

313
314
315 Figure 5. Enrichment of signatures of repeated association within genomic regions harbouring a
316 haploblock in one of the two compared lineages. Each panel shows the proportion of top
317 candidate genes that fall within haploblocks for windows with significant signatures of repeated
318 association by the null-W test (WRAs) vs. those with non-significant signatures (non-WRAs).
319 Comparisons of *H. petiolaris petiolaris* vs. *H. petiolaris fallax* are omitted as they share
320 segregating haploblocks. Each point corresponds to the results for a single phenotype or
321 environment, with dark shading used for cases where the deviation from random for the
322 contingency table is significant by a permutation test ($p < 0.05$), and lighter shading indicating a
323 non-significant result.
324
325

326 **Multi-species signatures of repeated association.** As a complement to the pair-wise analyses
327 described above, we also conducted an analysis using PicMin, which simultaneously considers
328 any number of lineages to identify genes with particularly strong and repeated signatures of
329 association (Booker et al. 2022). After clustering together windows < 1 Mbp apart, we found a
330 total of 145 regions that were significant for at least one variable or phenotype (at FDR < 0.1
331 applied within each variable). The largest number of significant regions for environment was
332 found with the Number of Frost-Free Days variable (20 with FDR < 0.1; 44 with FDR < 0.2) and
333 for phenotypes with Total Leaf Number (9 with FDR < 0.1; 19 with FDR < 0.2). Considering the
334 720 individual 5000 bp windows with FDR < 0.2 for at least one variable, 387 are within 500 bp
335 of a genic region, representing a 2.3x enrichment relative to the rate for windows that were not
336 significant hits using PicMin (23.3% of other windows fall within 500 bp of a genic region; X^2
337 test $p < 10^{-15}$).
338
339

340
341 **Estimating the number of potentially adaptive loci.** Even for the environment with the highest
342 repeatability (Number of frost-free days; NFFD), most of the strongest signals of association are
343 found in only one lineage (Figure 3B). This implies that there is considerable genotypic
344 redundancy, with many different ways for these species to adaptively respond to variation in the
345 same environment. To estimate the number of windows that could potentially contribute to local
346 adaptation for each variable (L_{eff}), we modified the method of Yeaman et al. (2018) to partially
347 account for the effect of linkage among nearby windows (see methods). This method assumes
348 that the windows with signatures of adaptation in each species are a random draw from a larger
349 number of potentially contributing windows (L_{eff}), which can be inferred based on the ratio of
350 shared vs. non-shared windows with strong association signatures (see Methods). We find that
351 estimates of L_{eff} tend to be large, always well over 1000 windows regardless of the trait or
352 environment (Figure S13A). There are numerous sources of error that affect the estimation of
353 L_{eff}, which will tend to be overestimated due to linkage (Figure S13A) or when many signatures
354 of adaptation are false positives (see supplementary results), and will be underestimated when
355 some repeatability is due to shared standing variation (Yeaman et al. 2018). Even after controls

356 for linkage and assuming a high false positive rate of 80%, estimates of L_{eff} remain in the
357 hundreds even for the variable with the lowest value of L_{eff} (Eref; Figure S13C, D).
358

359 **Discussion**

360 Despite its critical importance in shaping the architecture of adaptation, little is known about the
361 extent of genotypic redundancy underlying different traits (Barghi et al. 2020; Láruson et al.
362 2020; Yeaman 2022). Here, we have shown evidence of significant repeatability in the basis of
363 local adaptation (Figure 4, 5), but also an abundance of species-specific, non-repeated signatures
364 (Figure 3; S13). In particular, we find that regions of the genome that harbour inversions in one
365 species also tend to be strongly enriched for signatures of adaptation in other species lacking the
366 inversion (Figure 5). Taken together, this suggests that local adaptation in these species is highly
367 flexible -- different species apparently use quite different sets of loci to adapt to the same
368 environment -- yet still involves some component that has minimal redundancy, with inversions
369 playing a particularly important role. Some of the "usual suspects" show up in the set of
370 significantly repeated loci identified by PicMin: in addition to the homologs of the *FT*
371 (*FLOWERING LOCUS T*) gene reported by (Todesco et al. 2020), we also found hits for several
372 other genes involved in circadian regulation and flowering time, including *PRR3* (Para et al.
373 2007)), *TOE1* (Aukerman and Sakai 2003), and *PHYC* (Takano et al. 2005; Chen et al. 2014),
374 which is known to regulate photoperiodic responses in Arabidopsis accessions (Balasubramanian
375 et al. 2006). Other top hits included genes involved in plant development and auxin transport
376 (*PIN3*; (Keuskamp et al. 2010), *ARF4* (Pekker et al. 2005), and *MN*; (Bhatia et al. 2016)), and
377 plant immunity (*CRK13* (Acharya et al. 2007) and *PRR2* (Cheval et al. 2017))

378 The increased repeatability found in regions of the genome that harbour inversions in only
379 one species is particularly interesting. Inversions are commonly associated with local adaptation
380 (Wellenreuther and Bernatchez 2018), likely because they reduce the rate that recombination
381 breaks up combinations of co-selected alleles (Kirkpatrick and Barton 2006), which perhaps
382 facilitates contributions by alleles that would be individually too weakly selected to overcome
383 swamping by migration (Bürger and Akerman 2011; Yeaman and Whitlock 2011; Schaal et al.
384 2022). Evidence here suggests these regions still tend to contribute to adaptation in the species
385 lacking the recombination-suppressing effect of an inversion, consistent with a strong effect of

386 selection relative to migration on at least one locus in the region. Given that under this model,
387 inversions will be mostly likely to persist if they capture multiple locally adapted alleles, the
388 observation of enrichment of signatures of repeated adaptation within inversions could also
389 explain their long-term persistance. If there is variation across the genome in the density of loci
390 with the potential to be involved in local adaptation, then the evolution and maintenance of
391 locally adaptive inversions would be biased towards co-occuring with the loci most likely to be
392 involved in local adaptation. If the potential for local adaptation is conserved amongst species,
393 then these same regions are more likely to have high repeatability. In this way, repeatability in
394 inversion containing regions may reflect the preferential retention of inversions, as well as the
395 retention of locally adaptive alleles. As an example, chromosome 15 harbours a large (72 Mbp)
396 haploblock in *H. annuus* that is strongly associated with NFFD (number of frost-free days), and
397 also shows some signatures of association in the other taxa, with particularly strong signatures of
398 association on either side of the haploblock in *H. argophyllus* (Figure 3A). Interestingly, loci of
399 repeated association identified by PicMin within this region include two genes whose homologs
400 are known to regulate responses to cold: *COLD-RESPONSIVE PROTEIN KINASE 1*,*CRPK1*
401 (Liu et al. 2017)) and *LATE ELONGATED HYPOCOTYL*, *LHY* (Mizoguchi et al. 2002; Dong et
402 al. 2011). While many studies have demonstrated the importance of inversions for adaptation
403 (Wellenreuther and Bernatchez 2018; Hager et al. 2022), to our knowledge only one other study
404 has documented the involvement of the same loci making contributions in the absence of the
405 recombination-suppressing effect of the inversion (Lee et al. 2017). This also highlights how
406 comparative studies of a species lacking an inversion may help identify which genes are driving
407 adaptation in another species with an inversion, as segregating inversions tend to have extensive
408 LD that prevents identification of any potential targets of natural selection within them.

409 While our results suggest a large number of loci can potentially contribute to adaptation,
410 implying high redundancy (Figure 3B; S13), there are several factors that complicate inference.
411 Separating the effects of drift and selection to detect signatures of local adaptation is notoriously
412 difficult, because population structure often covaries with features of the environment that drive
413 adaptation (Lotterhos and Whitlock 2014; Hoban et al. 2016; DeRaad et al. 2021). As found by
414 other analyses (Yeaman et al. 2016; DeRaad et al. 2021), when we use structure correction in our
415 genotype-environment association tests, we find many fewer signatures of repeated association

416 (Figure S6 vs. S8), likely due to the reduced power of Baypass to detect true positives when the
417 environment covaries with population structure. Here, we have side-stepped the issues involved
418 in correction for population structure by instead relying on comparisons among species to
419 identify loci with associations more extreme than expected by chance, using the null-W and
420 PicMin tests. This assumes that most loci in the genome are not involved in local adaptation, so
421 that the relatively small proportion that are driving adaptation can therefore be picked out due to
422 their tendency to fall into the tail of the distribution of association statistics. While this approach
423 should be relatively robust for identifying loci with repeated patterns of adaptation, there is no
424 way to formally estimate significance of associations found in only a single species, many of
425 which may be false positives due to covariation of population structure and environment.
426 However, even if we assume that 80% of the observed non-repeated loci are false positives, we
427 still find that estimates of the effective number of loci contributing to adaptation (L_{eff}) are in the
428 hundreds (Figure S13C). As we are unable to detect loci of small effect due to the limited power,
429 our estimates of L_{eff} will also be biased downwards by excluding these potentially important
430 drivers. Finally, it is also difficult to exclude the contribution of introgression or incomplete
431 lineage sorting to the observed signatures repeated association. If a locus tended to be highly
432 introgressed between two species in a restricted region of their range, it is possible it could also
433 covary with environment and therefore result in a signature of repeated association that would be
434 mistakenly interpreted as adaptation. While it is difficult to preclude this from our analysis,
435 regions of the genome with signatures of repeated association do not tend to have higher levels
436 of shared standing variation than background regions (Figure S5), suggesting this is not a broad
437 explanation for our observations. If anything, shared standing variation would be expected to
438 increase repeatability of adaptation (MacPherson and Nuismer 2017), adding further weight to
439 the inference that there is high genotypic redundancy in these species.

440 In general, we find that temperature is the strongest driver of repeated adaptation at both
441 the phenotypic and genomic levels. We quantified local adaptation at the phenotypic level using
442 correlations between traits measured in common gardens and the home environment of the
443 population they were sampled from. Across all phenotypes, these correlations tended to be
444 strongest and most similar among species for temperature variables, particularly in comparisons
445 among *H. annuus* and *H. petiolaris* subspecies (Figure S2). We see similar patterns of

446 repeatability reflected in the genome, where temperature variables also tend to have the greatest
447 repeatability (Figure 4). The similarity in these phenotypic and genomic signatures is consistent
448 with an effect of strong selection, as other artefactual or drift-based explanations for repeatability
449 would not be expected to reflect patterns found at the phenotypic level. It should be noted that
450 the reduced importance of soil variables in the SIPEC index might be partly driven by the fact
451 that all traits were measured on above-ground features, due to the difficulty of getting good root
452 phenotypes.

453 Taken together, these results suggest that some fraction of the genome contributes to adaptation
454 with low redundancy and high repeatability (which tend to be enriched within inversions), while
455 the remainder of the adaptive response is driven by loci with high redundancy and species-
456 specific contributions. Models in evolutionary genetics tend to focus on extremes: population
457 genetic approaches explore cases where strong selection deterministically drives a change in
458 allele frequency, whereas quantitative genetic approaches make the infinitesimal assumption that
459 phenotypic change can be realized through small frequency changes at many loci (Barton et al.
460 2017; Barghi et al. 2020; Yeaman 2022). Our results suggest that adaptation is a complex
461 process that does not map cleanly onto the assumptions of either approach, but that at least some
462 component of trait variation experiences sufficiently strong selection to overcome migration and
463 drift and behave in a way approximately consistent with population genetic models. Given the
464 difficulty of rigourously quantifying the contribution of alleles of small effect, it remains an open
465 question what proportion of adaptive response is governmed by loci with dynamical behaviour
466 that follow the infinitesimal assumption. This could perhaps be quantified explicitly by
467 decomposing trait heritabilities as has been done for standing variation in humans (Visscher et al.
468 2017), but this would require a considerable increase in sample size as methods such as GCTA
469 (Yang et al. 2011) do not yield accurate estimates at the sample sizes used here

470

471 **Materials and Methods**

472 **Data collection, common garden, and phenotyping.** Seed samples were collected from 151
473 wild sunflower populations covering most of their native distributions during the summer of
474 2015 (*H. annuus*: 61 populations for GWAS and 71 populations for GEA, *H. petiolaris fallax*: 23

475 populations, *H. petiolaris petiolaris:* 18 populations and *H. argophyllus*: 30 populations, Figure
476 1 and Supplementary Table 1). Seeds from ten additional populations of *H. annuus* for the GEA
477 analysis had been previously collected in the summer of 2011. Sample seeds were obtained from
478 randomly chosen mothers, and were first germinated in a greenhouse for two weeks, later moved
479 to an open-sided greenhouse for acclimation. Phenotypic data were collected throughout the
480 growing season, as detailed in Supplementary Table 1. Extensive records of developmental and
481 morphological traits throughout the growth of the plants including leaves, stem, and seeds which
482 were collected and digitally imaged to extract relevant phenotypic data.
483
484 **Similarity in Phenotype-Environment Correlation (SIPEC).** Locally adapted traits tend to
485 exhibit strong correlations between environment and common-garden phenotype, so
486 environments that are important to driving local adaptation should exhibit strong correlations
487 with many traits. As an index to represent the similarity among pairs of species in an
488 environment's average correlation across all measured phenotypes, we calculate SIPEC =
489 $\sum_i \left(|r_{i,1}| + |r_{i,2}|\right)|r_{i,1}||r_{i,2}|/n_p$ where $r_{i,1}$ and $r_{i,2}$ are the Pearson correlations between the
490 environment and the ith phenotype in the first and second species, respectively, and n_p is the
491 number of phenotypes. This SIPEC index is maximized when the correlation is large in both
492 species regardless of the direction, so it does not differentiate phenotypically convergent vs.
493 divergent patterns of local adaptation, and provides a means of estimating the relative importance
494 of an environment driving local adaptation across all measured phenotypes. To account for non-
495 independence among traits, for each pair of species we fit a PCA to all measured phenotypes and
496 use the Principal Components that collectively explain 95% of the variance, and calculate SIPEC
497 on the correlations of these variables with environment.

498

499 **Tests of SNP association with environment (GEA) and phenotype (GWAS).** A total of 39
500 environmental variables (21 climatic variables, 3 geographic variables, 15 soil variables
501 Supplementary Table 1) were used for the genotype-environment association analysis (GEA).
502 We refer to the climatic, soil and geographic variables collectively as the "environmental
503 variables", for simplicity. Soil data were collected by taking three to five soil samples collected
504 at each population from across the area in which seeds were collected and submitted to Midwest

505 Laboratories Inc. (Omaha, NE, USA) for analysis. Climate data for each population were
506 collected over a 30-year period (1961-1990) from geographic coordinates of the locations where
507 the samples were collected, using the software package Climate NA (Wang et al. 2012). We used
508 the package BAYPASS version 2.1 (Gautier 2015), which provides a re-implementation of the
509 Bayesian hierarchical model, and explicitly accounts for the covariance structure among the
510 population allele frequencies that originate from the shared history of the populations through the
511 estimation of the population covariance matrix. This renders the identification of SNPs subjected
512 to selection less sensitive to the confounding effect of population demography (Günther and
513 Coop 2013). Population structure was estimated by choosing a random and unlinked set of 10 kb
514 SNPs and running BAYPASS under the core model (*i.e.* no covariates). Then the Bayes factors
515 (BF) were calculated running BAYPASS under the STD covariate model to evaluate association
516 of SNPs with environmental variables (*i.e*. adjusting for population structure). For each SNP, the
517 Bayes factor (denoted BF_{is} as in Gautier 2015) was presented in decibian units (db) via the
518 transformation 10 $\log_{10}$ (BF). BF_{is} relies on the importance sampling algorithm proposed by
519 Coop et al., 2010 and uses MCMC samples obtained under the core model. To produce a
520 narrower set of outlier loci, we followed the popular Jeffreys' rule (Jeffreys 1961) that identified
521 outlier loci with BF $\geq$ 10. As genome scan methods that correct for population structure can
522 remove some potential signals of local adaption when there is covariation between the
523 demographic history of the species and the environmental variables or phenotypic traits of
524 interest, we also calculated Spearman's rank correlation (ρ, uncorrected GEA) between
525 population allele frequencies for each SNP and each environment variable.
526 GWAS analysis was performed 86, 30 and 69 developmental and morphologic traits in *H.*
527 *annuus, H. argophyllus* and *H. petiolaris,* respectively (Supplementary table 1). 29 variables
528 were measured in all three focal species, and 39 were measured only in *H. annuus* and in *H.*
529 *petiolaris* subspecies (Supplementary table 1). Seed and flower traits could not be collected for
530 *H. argophyllus*, since most plants of this species flowered very late in our common garden, and
531 failed to form fully developed inflorescences and set seeds before temperatures became too low
532 for their survival. Population structure was controlled for in GWAS by including the first three
533 principal components as covariates, as well as an identity-by-state (IBS) kinship matrix
534 calculated by EMMAX (Kang et al. 2010). We ran each trait GWAS using EMMAX
535 (v07Mar2010), as well as the EMMAX module in EasyGWAS (Grimm et al. 2017). For every

536 SNP/peak above the Bonferroni significance threshold, candidate genes were selected within a
537 100 Kb interval centered in the SNP with the lowest p-value, or within the boundaries of the
538 GWAS peak, whichever was larger. All variants used for association were initially filtered for
539 VQSR 90% tranche, and then further filtered to only include bi-allelic SNPs genotyped in ≥ 90%
540 of samples and with a minor allele frequency ≥ 3%.

541 **Identification of top-candidate windows.** We calculated the bottom 0.01 quantiles for the *p*-
542 values from association tests, Spearman's rank correlation (uncorrected GEA) and GWAS
543 (corrected and uncorrected), yielding two 1% cutoffs. For each environmental and phenotypic
544 variable, we identified all outlier SNPs as those that fell below the respective 1% cutoff. For
545 BayPass, we considered SNPs with Bayes factor ≥ 10 as outlier SNPs. For each 5 kb window
546 that we defined across the whole genome, we counted the number of outlier SNPs (a) and the
547 total number of SNPs (n). To identify top-candidate windows for each variable, we compared the
548 number of outlier SNPs per each 5 kb window to the 0.9999 quantile of the binomial expectation
549 where the expected frequency of outlier SNPs per window is calculated as: $\rho = \sum a_i/n_i$
550 (summation over all 5 kp windows), calculating ρ independently for each environmental and
551 phenotype variable and excluding windows with 0 outliers from the calculation of ρ (as per
552 Yeaman et al. 2016). We also calculated a top candidate index using the same approach to
553 categorize outliers, obtaining a *p*-value for a binomial test for the number of SNPs per window
554 given an expected proportion of outliers (ρ; this *p*-value is not exact due to non-independence of
555 SNPs so we refer to this as an index).

556 Identifying outlier SNPs detected by genome scans from genome-wide distribution without
557 accounting for local recombination rate variation can promote false positive signals in
558 recombination cold spots (i.e., low recombination regions) and be overly conservative in
559 recombination hot spots (i.e., high recombination regions) (Booker et al. 2020). Therefore, to
560 account for local recombination rate variation, all genomic windows were binned by their
561 estimated recombination rates into 5 equally sized bins (bin1: 0-20% quantile, bin2: 20%-40%
562 quantile, bin3: 40%-60% quantile, bin4: 60%-80% quantile, bin5: 80%-100% quantile). For each
563 recombination bin, we estimated expected frequency of SNPs per window (ρ) and calculated cut-
564 off separately. Windows falling above the threshold were identified as top candidate windows.

565 **Genome-wide survey of repeatability (null-W test).** To explore repeatable genomic signatures
566 of adaptation for each of the six pairwise contrasts among the 4 taxa (Figure 1), we used the
567 method developed by Yeaman et al. (2016) with some modifications. A common approach is to
568 identify candidates for adaptation independently in each species and then examine the overlap
569 between these lists, however this approach is quite stringent and may miss many interesting
570 signals. The null-W test is more sensitive, as it takes the list of top candidates from one species
571 and tests whether they tend to show more extreme signatures of association than expected by
572 chance. The null-W test is especially favorable when LD increased divergence of SNPs in tight
573 linkage with casual SNPs but did not raise the test values enough for a window to be classified as
574 an outlier according to the binomial test. For each top candidate window that we identified for
575 each focal species in a pair, we refer to the same window in the other species as "top candidate
576 ortholog". The null distribution for each focal species and variable was constructed by randomly
577 sampling 10,000 background SNPs from non-top candidate ortholog windows. For each non-top-
578 candidate window, we then estimated the test statistic (*W*) for the Wilcoxon-signed rank test vs.
579 the 10,000 background SNPs. This resulted in a null distribution representing the differences
580 between the 10,000 background SNPs and the non-top-candidate ortholog windows. These were
581 then standardized to *Z*-scores using the method in Whitlock and Schluter (2020):

582 $$Z = \frac{2W - n1n2}{\sqrt{n1n2(n1+n2+1)/3}} \qquad \text{(Equation 2)}$$

583

584 where n1 and n2 are the sample sizes being compared. In order to control for heterogeneity in
585 recombination rate and its possible effects on the null distribution, we estimated null distribution
586 for each recombination bin separately (5 in total, see above). We then compared the p-values and
587 bayes factors (BFs) for each focal top-candidate widow to the 10,000 background SNPs,
588 calculating the W statistics and converting into a Z-score. Empirical P-values were then
589 calculated by comparing the Z-score for each top-candidate window to the null distribution.
590 When individual windows had values of W that exceeded the bounds of the null distribution,
591 their empirical *p*-value was set to the reciprocal of the number of genes in the null distribution.
592 Empirical *p*-values were converted to *q*-values for estimation of False Discovery Rate and
593 applied this separately to the empirical p-values for each of the variables. For each species pair,

594 we refer to the windows identified as significant by this test as "Windows of Repeated
595 Association" or WRAs.

596

597 **Linkage disequilibrium and detection of clusters of repeated association.** Linkage
598 disequilibrium among adjacent genomic windows can result in statistical non-independence and
599 similar GEA/GWAS signatures across many windows. To group neighbouring WRAs with
600 similar signatures of repeatability into a single "Cluster of Repeated Association" (CRA), we
601 used the following approach in each pairwise contrast, and for each environmental variable and
602 phenotype: beginning with the first WRA along the chromosome, we compared it to the next
603 closest WRA by calculating the Pearson correlation coefficient (r^2) on the allele frequencies
604 across all pairs of SNPs, and compared this estimate to a null distribution. To construct the null
605 distribution, we generated a distribution of LD measurements between 10,000 randomly chosen
606 windows with the same physical distance as between two WRAs (excluding all WRAs from the
607 null distribution). If the r^2 between the two neighboring WRAs was greater than the 95th
608 percentile of the null distribution, we clustered these two windows together. This process was
609 repeated successively with the next closest neighboring WRA, walking out along the
610 chromosome until one of two stopping criteria was reached: 1) the LD between the last two
611 windows did not exceed the 95 percent of the tail distribution or 2) the distance between the
612 initial window and the current window next to it was larger than 1 cM, based on the linkage map
613 from Todesco et al. (2020). When the first round of clustering stopped due to either of these two
614 criteria, all the clustered windows were removed from the dataset and the process started with the
615 second smallest empirical p-value. By doing this way, each WRA will only appear in a single
616 CRA.
617

618 **Estimating an index of shared standing variation.** As genotype calling was conducted
619 separately for each species (due to computational concerns), we estimated the amount of shared
620 standing variation based on counts of shared vs. non-shared SNPs. If two species are evolving
621 independently, the number of shared SNPs should follow a hypergeometric distribution, so we
622 used an approach similar to the C-scores (Yeaman et al. 2018) to calculate the difference
623 between the observed number of shared SNPs and the expectation, scaled by the standard

624 deviation of the hypergeometric. Because of noise and a relatively small number of SNPs per
625 window, we applied this approach on a sliding window basis, including the 5 flanking windows
626 upstream and downstream of each focal window the calculation of its index of shared standing
627 variation.

628 **Correspondence between regions of repeated association and chromosomal**
629 **rearrangements.** To assess the extent of overlap between regions of the genome with repeated
630 signatures of association and previously identified low-recombination haploblocks, we used two
631 approaches. Firstly, for each pairwise species contrast and variable, we constructed a
632 contingency table for the number of top candidates that were significant WRAs vs. not-
633 significant WRAs (by the null-W test), and that did vs. did not fall within a haploblock. We
634 calculated the Pearson's χ^2 statistic on this table, and then permuted the location of haploblocks
635 throughout the genome to construct a null distribution of χ^2 statistics, and calculated the p-value
636 as the proportion of the null that exceeded the observed χ^2 statistic (to account for non-
637 independence of nearby WRAs). Secondly, we compared observations of the length and number
638 of overlapping regions to expectations based on a randomization approach. For each pair of
639 species, we kept the position of each CRA constant and randomized the position of haploblocks
640 10,000 times to build a null distribution. By keeping the position of the CRAs constant, we
641 maintained the architecture of adaptation independent from chromosomal rearrangements. We
642 assessed significance by testing whether the observed overlaps between CRAs and haploblocks
643 were more extreme than the 95th percentile of the tail of null distribution. Details about
644 identifying chromosomal rearrangements can be found in Todesco et al. (2020).

645 **Identifying repeated signatures of association across all taxa**. As a complement the the
646 pairwise analysis, we used PicMin (Booker et al. 2022) to identify windows of the genome with
647 strong signatures of association in multiple (sub-) species. For each environmental variable,
648 association signatures for each window are ranked genome-wide and PicMin identifies windows
649 with extreme ranks in multiple species. We ran the analysis once with each of the two 3-way
650 comparisons involving one *petiolaris* subspecies (i.e. *H. annuus, H. argophyllus,* and either *H.*
651 *pet. petiolaris* or *H. pet. fallax*) to control for repeatability arising from similar patterns in the
652 two *petiolaris* subspecies (due to high introgression/shared standing variation).

653 **Evaluating genotypic redundancy using C-scores.** Genome-wide quantification of the
654 repeatability of association statistics provides insights into the amount of genotypic redundancy
655 underlying a trait or environmental adaptation, and can be assessed using the C-score approach
656 (Yeaman et al. 2018). Briefly, for a given trait or environment, the set of association test scores
657 within each species is classified into "associated" or "non-associated" using the binomial top
658 candidate approach. For a given pair of species (i = 1, 2), the observed number of associated
659 windows in each species (a_1, a_2) can be compared to the number of windows that are associated
660 in both species (a_b) and the total number of windows being analysed (a_x). Under a null
661 hypothesis where all windows in the genome have equal potential to be involved in adaptation
662 (i.e. associated with the trait or environment), the expected number of windows associated in
663 both species will be described by a hypergeometric distribution, with the expectation $\overline{a_b} =$
664 $a_1 a_2 / a_x$. The difference between the observed and expected amount of overlap in association
665 scores can be quantified as a C-score by scaling the difference by the standard deviation of the
666 hypergeometric (i.e. a C-score of 2 means that the observed amount of overlap is two standard
667 deviations above the expectation under randomness).
668 We assess the C-scores for each phenotype and environment trait by classifying the top
669 0.5% of all 5 kb windows within each species as "associated" (a_i; based on the binomial top
670 candidate index), and begin by calculating the C-score obtained when a_x is set to the union of a_i
671 across all four focal species/sub-species (i.e. only those windows associated in at least one
672 species are included in a_x, a number much lower than the total number of windows in the
673 genome). This yields a negative C-score, as a random draw from such a small number of
674 windows tends to yield many more overlapping associations by chance than the observation.
675 When the C-score = 0, it means that the observed overlap between the pair of taxa being
676 considered is consistent with a random draw of their respective "associated" windows from an
677 overall pool of a_x windows. Thus, by adding rows to the matrix with "non-associated" scores for
678 all 4 species/sub-species until finding the matrix that yields C-score = 0, we can estimate the
679 effective number of loci that contributed to variation for the trait or environment being
680 considered (L_{eff}), under the assumption that all such $a_x = L_{eff}$ windows had an equal chance of
681 contributing to the associations.
682 To run the C-score analysis on LD-clustered windows, we ran the following algorithm for
683 each trait/environmental variable: for each species, we identified all CRAs that also had a top

candidate index in top 0.5%. In most cases, a large cluster with associated windows in one species corresponds to either no clusters or a small cluster in another species. To harmonize cluster boundaries across species, we bin any overlapping clusters together to their maximum extent, and take the average top candidate index for each cluster in each species as either: (a) the mean across all windows that were "associated" in that species or (b) the average across all windows associated in any species, if no windows were associated in that species. This yields a matrix that can be submitted to the hypergeometric C-score analysis.

Data availability

All scripts used for analysis and figures will be deposited in a Dryad archive along data files and results. Raw sequence data are deposited in the Sequence Read Archive (SRA) under BioProject accessions PRJNA532579, PRJNA398560, and PRJNA564337, as described in Todesco et al. (2020).

Acknowledgements:

The authors would like to thank the Yeaman and Peichel labs for comments. Computational support was provided by the Digital Resources Alliance of Canada, and funding was provided by Genome Canada and Genome BC (LSARP2014-223SUN) and the International Consortium for Sunflower Genomic Resources. SY was funded by Alberta Innovates and NSERC Discovery. GLO was funded by a Banding Postdoctoral Fellowship.

References:

Acharya BR, Raina S, Maqbool SB, Jagadeeswaran G, Mosher SL, Appel HM, Schultz JC, Klessig DF, Raina R. 2007. Overexpression of CRK13, an Arabidopsis cysteine-rich receptor-like kinase, results in enhanced resistance to Pseudomonas syringae: Overexpression of CRK13 induces pathogen defense. *The Plant Journal* 50:488–499.

Auge GA, Penfield S, Donohue K. 2019. Pleiotropy in developmental regulation by flowering-pathway genes: is it an evolutionary constraint? *New Phytol* 224:55–70.

Aukerman MJ, Sakai H. 2003. Regulation of Flowering Time and Floral Organ Identity by a MicroRNA and Its *APETALA2* -Like Target Genes. *Plant Cell* 15:2730–2741.

Balasubramanian S, Sureshkumar S, Agrawal M, Michael TP, Wessinger C, Maloof JN, Clark R, Warthmann N, Chory J, Weigel D. 2006. The PHYTOCHROME C photoreceptor gene mediates natural variation in flowering and growth responses of Arabidopsis thaliana. *Nat Genet* 38:711–715.

Barghi N, Hermisson J, Schlötterer C. 2020. Polygenic adaptation: a unifying framework to understand positive selection. *Nat Rev Genet* 21:769–781.

Barton NH, Etheridge AM, Véber A. 2017. The infinitesimal model: Definition, derivation, and implications. *Theoretical Population Biology* 118:50–73.

Bhatia N, Bozorg B, Larsson A, Ohno C, Jönsson H, Heisler MG. 2016. Auxin Acts through MONOPTEROS to Regulate Plant Cell Polarity and Pattern Phyllotaxis. *Current Biology* 26:3202–3208.

Blackman BK, Scascitelli M, Kane NC, Luton HH, Rasmussen DA, Bye RA, Lentz DL, Rieseberg LH. 2011. Sunflower domestication alleles support single domestication center in eastern North America. *Proc. Natl. Acad. Sci. U.S.A.* 108:14360–14365.

Bohutínská M, Vlček J, Yair S, Laenen B, Konečná V, Fracassetti M, Slotte T, Kolář F. 2021. Genomic basis of parallel adaptation varies with divergence in *Arabidopsis* and its relatives. *Proc. Natl. Acad. Sci. U.S.A.* 118:e2022713118.

Booker TR, Yeaman S, Whitlock MC. 2020. Variation in recombination rate affects detection of outliers in genome scans under neutrality. *Mol Ecol* 29:4274–4279.

Booker TR, Yeaman S, Whitlock MC. 2022. Using genome scans to identify genes used repeatedly for adaptation. Evolutionary Biology Available from: http://biorxiv.org/lookup/doi/10.1101/2022.03.24.485690

Bürger R, Akerman A. 2011. The effects of linkage and gene flow on local adaptation: A two-locus continent–island model. *Theoretical Population Biology* 80:272–288.

741 Chen A, Li C, Hu W, Lau MY, Lin H, Rockwell NC, Martin SS, Jernstedt JA, Lagarias JC,
742 Dubcovsky J. 2014. PHYTOCHROME C plays a major role in the acceleration of wheat
743 flowering under long-day photoperiod. *Proc. Natl. Acad. Sci. U.S.A.* 111:10037–10044.

744 Cheval C, Perez M, Leba LJ, Ranty B, Perochon A, Reichelt M, Mithöfer A, Robe E, Mazars C,
745 Galaud JP, et al. 2017. PRR2, a pseudo-response regulator, promotes salicylic acid and
746 camalexin accumulation during plant immunity. *Sci Rep* 7:6979.

747 DeRaad DA, Cobos ME, Alkishe A, Ashraf U, Ahadji-Dabla KM, Nuñez-Penichet C, Peterson
748 AT. 2021. Genome-environment association methods comparison supports omnigenic
749 adaptation to ecological niche in malaria vector mosquitoes. *Molecular Ecology*
750 30:6468–6485.

751 Dong MA, Farré EM, Thomashow MF. 2011. CIRCADIAN CLOCK-ASSOCIATED 1 and
752 LATE ELONGATED HYPOCOTYL regulate expression of the C-REPEAT BINDING
753 FACTOR (CBF) pathway in *Arabidopsis*. *Proc. Natl. Acad. Sci. U.S.A.* 108:7241–7246.

754 Gautier M. 2015. Genome-Wide Scan for Adaptive Divergence and Association with
755 Population-Specific Covariates. *Genetics* 201:1555–1579.

756 Grimm DG, Roqueiro D, Salomé PA, Kleeberger S, Greshake B, Zhu W, Liu C, Lippert C,
757 Stegle O, Schölkopf B, et al. 2017. easyGWAS: A Cloud-Based Platform for Comparing
758 the Results of Genome-Wide Association Studies. *Plant Cell* 29:5–19.

759 Günther T, Coop G. 2013. Robust Identification of Local Adaptation from Allele Frequencies.
760 *Genetics* 195:205–220.

761 Hager ER, Harringmeyer OS, Wooldridge TB, Theingi S, Gable JT, McFadden S, Neugeboren
762 B, Turner KM, Jensen JD, Hoekstra HE. 2022. A chromosomal inversion contributes to
763 divergence in multiple traits between deer mouse ecotypes. *Science* 377:399–405.

764 Heiser C, Smith D, Clevenger S, Martin W. 1969. The North American sunflowers (Helianthus).
765 *Memoirs of the Torrey Botanical Club* 22:1–218.

766 Heiser, CB. 1951. Hybridization in the Annual Sunflowers: Helianthus annuus x H. argophyllus.
767 *The American Naturalist* 85:65–72.

768 Hoban S, Kelley JL, Lotterhos KE, Antolin MF, Bradburd G, Lowry DB, Poss ML, Reed LK,
769 Storfer A, Whitlock MC. 2016. Finding the Genomic Basis of Local Adaptation: Pitfalls,
770 Practical Solutions, and Future Directions. *The American Naturalist* 188:379–397.

771 Izawa T. 2007. Adaptation of flowering-time by natural and artificial selection in Arabidopsis
772 and rice. *Journal of Experimental Botany* 58:3091–3097.

773 Jeffreys H. 1961. Theory of probability. 3rd ed. New York, NY: Oxford University Press

774 Kang HM, Sul JH, Service SK, Zaitlen NA, Kong S, Freimer NB, Sabatti C, Eskin E. 2010.
775 Variance component model to account for sample structure in genome-wide association
776 studies. *Nat Genet* 42:348–354.

777 Keuskamp DH, Pollmann S, Voesenek LACJ, Peeters AJM, Pierik R. 2010. Auxin transport
778 through PIN-FORMED 3 (PIN3) controls shade avoidance and fitness during
779 competition. *Proc. Natl. Acad. Sci. U.S.A.* 107:22740–22744.

780 Kirkpatrick M, Barton N. 2006. Chromosome Inversions, Local Adaptation and Speciation.
781 *Genetics* 173:419–434.

782 Láruson ÁJ, Yeaman S, Lotterhos KE. 2020. The Importance of Genetic Redundancy in
783 Evolution. *Trends in Ecology & Evolution* 35:809–822.

784 Lee C-R, Wang B, Mojica JP, Mandáková T, Prasad KVSK, Goicoechea JL, Perera N, Hellsten
785 U, Hundley HN, Johnson J, et al. 2017. Young inversion with multiple linked QTLs
786 under selection in a hybrid zone. *Nat Ecol Evol* 1:0119.

787 Liu Z, Jia Y, Ding Y, Shi Y, Li Z, Guo Y, Gong Z, Yang S. 2017. Plasma Membrane CRPK1-
788 Mediated Phosphorylation of 14-3-3 Proteins Induces Their Nuclear Import to Fine-Tune
789 CBF Signaling during Cold Response. *Molecular Cell* 66:117-128.e5.

790 Lotterhos KE, Whitlock MC. 2014. Evaluation of demographic history and neutral
791 parameterization on the performance of F_{ST} outlier tests. *Mol Ecol* 23:2178–2192.

792 MacPherson A, Nuismer SL. 2017. The probability of parallel genetic evolution from standing
793 genetic variation. *J. Evol. Biol.* 30:326–337.

794 Manceau M, Domingues VS, Linnen CR, Rosenblum EB, Hoekstra HE. 2010. Convergence in
795 pigmentation at multiple levels: mutations, genes and function. *Phil. Trans. R. Soc. B*
796 365:2439–2450.

797 Mizoguchi T, Wheatley K, Hanzawa Y, Wright L, Mizoguchi M, Song HR, Carré IA, Coupland
798 G. 2002. LHY and CCA1 are partially redundant genes required to maintain circadian
799 rhythms in Arabidopsis. *Dev Cell* 2:629–641.

800 Moyers BT, Rieseberg LH. 2016. Remarkable life history polymorphism may be evolving under
801 divergent selection in the silverleaf sunflower. *Mol Ecol* 25:3817–3830.

802 Ostevik KL, Andrew RL, Otto SP, Rieseberg LH. 2016. Multiple reproductive barriers separate
803 recently diverged sunflower ecotypes: reproductive barriers between sunflower ecotypes.
804 *Evolution* 70:2322–2335.

805 Para A, Farré EM, Imaizumi T, Pruneda-Paz JL, Harmon FG, Kay SA. 2007. PRR3 Is a vascular
806 regulator of TOC1 stability in the Arabidopsis circadian clock. *Plant Cell* 19:3462–3473.

807 Pekker I, Alvarez JP, Eshed Y. 2005. Auxin response factors mediate Arabidopsis organ
808 asymmetry via modulation of KANADI activity. *Plant Cell* 17:2899–2910.

809 Rosenblum EB, Parent CE, Brandt EE. 2014. The Molecular Basis of Phenotypic Convergence.
810 *Annu. Rev. Ecol. Evol. Syst.* 45:203–226.

811 Sambatti JBM, Strasburg JL, Ortiz-Barrientos D, Baack EJ, Rieseberg LH. 2012. Reconciling
812 extremely strong barriers with high levels of gene exchange in annual sunflowers: gene
813 flow across a strong reproductive barrier. *Evolution* 66:1459–1473.

814 Schaal SM, Haller BC, Lotterhos KE. 2022. Inversion invasions: when the genetic basis of local
815 adaptation is concentrated within inversions in the face of gene flow. *Phil. Trans. R. Soc.*
816 *B* 377:20210200.

817 Strasburg JL, Rieseberg LH. 2008. Molecular demographic history of the annual sunflowers
818 *helianthus annuus* and *h. Petiolaris* -large effective population sizes and rates of long-
819 term gene flow. *Evolution* 62:1936–1950.

820 Takano M, Inagaki N, Xie X, Yuzurihara N, Hihara F, Ishizuka T, Yano M, Nishimura M,
821 Miyao A, Hirochika H, et al. 2005. Distinct and Cooperative Functions of Phytochromes
822 A, B, and C in the Control of Deetiolation and Flowering in Rice. *The Plant Cell*
823 17:3311–3325.

824 Tittes S, Lorant A, McGinty S, Doebley JF, Holland JB, Sánchez-González J de J, Seetharam A,
825 Tenaillon M, Ross-Ibarra J. 2021. Not so local: the population genetics of convergent
826 adaptation in maize and teosinte. Evolutionary Biology Available from:
827 http://biorxiv.org/lookup/doi/10.1101/2021.09.09.459637

828 Todesco M, Owens GL, Bercovich N, Légaré J-S, Soudi S, Burge DO, Huang K, Ostevik KL,
829 Drummond EBM, Imerovski I, et al. 2020. Massive haplotypes underlie ecotypic
830 differentiation in sunflowers. *Nature* 584:602–607.

831 Visscher PM, Wray NR, Zhang Q, Sklar P, McCarthy MI, Brown MA, Yang J. 2017. 10 Years
832 of GWAS Discovery: Biology, Function, and Translation. *The American Journal of*
833 *Human Genetics* 101:5–22.

834 Wang L, Josephs EB, Lee KM, Roberts LM, Rellán-Álvarez R, Ross-Ibarra J, Hufford MB.
835 2021. Molecular Parallelism Underlies Convergent Highland Adaptation of Maize
836 Landraces.Purugganan M, editor. *Molecular Biology and Evolution* 38:3567–3580.

837 Wang T, Hamann A, Spittlehouse DL, Murdock TQ. 2012. ClimateWNA—High-Resolution
838 Spatial Climate Data for Western North America. *Journal Of Applied Meteorology And*
839 *Climatology* 51:14.

840 Wellenreuther M, Bernatchez L. 2018. Eco-Evolutionary Genomics of Chromosomal Inversions.
841 *Trends in Ecology & Evolution* 33:427–440.

842 Whitlock M, Schluter D. 2020. The analysis of biological data. 3rd ed. Macmillan

843 Yang J, Lee SH, Goddard ME, Visscher PM. 2011. GCTA: A Tool for Genome-wide Complex
844 Trait Analysis. *The American Journal of Human Genetics* 88:76–82.

845 Yeaman S. 2022. Evolution of polygenic traits under global *vs* local adaptation. *Genetics*
846 220:iyab134.

847 Yeaman S, Gerstein AC, Hodgins KA, Whitlock MC. 2018. Quantifying how constraints limit
848 the diversity of viable routes to adaptation.Ralph PL, editor. *PLoS Genet* 14:e1007717.

849 Yeaman S, Hodgins KA, Lotterhos KE, Suren H, Nadeau S, Degner JC, Nurkowski KA, Smets
850 P, Wang T, Gray LK, et al. 2016. Convergent local adaptation to climate in distantly
851 related conifers. *Science* 353:1431–1433.

852 Yeaman S, Whitlock MC. 2011. The genetic architecture of adaptation under migration-selection
853 balance: the genetic architecture of local adaptation. *Evolution* 65:1897–1911.

854

855